Title: Scaffolds of 1, 2, 4, triazolo [1, 5-a] pyrimidin-7-amine as potential inhibitors of *Plasmodium falciparum* dihydroorotate dehydrogenase: Fragment-Based Drug Design, 2D-QSAR and DFT Calculation

Authors: Opeyemi Iwaloye[1*], Olusola Olalekan Elekofehinti[1], Femi Olawale[2, 3], Prosper Obed Chukwuemeka[4], Kikiowo Babatomiwa[5], Ibukun Mary Folorunso[1]

[1]Bioinformatics and Molecular Biology Unit, Department of Biochemistry, Federal University of Technology Akure, Ondo State, P.M.B. 704, Akure, 360001 Nigeria.

popenapoleon@gmail.com, ooelekofehinti@futa.edu.ng, folorunsoibukun43@gmail.com

[2]Nano-Gene and Drug Delivery Group, Department of Biochemistry, School of life science, University of Kwazulu Natal, 4000, Durban, South Africa. olawalefemi3@gmail.com

[3]Department of Biochemistry, University of Lagos, Nigeria

[4]Federal University of Technology Akure, Ondo State, P.M.B. 704, Akure, 360001 Nigeria.

Chukwuemekamcb154271@futa.edu.ng

[5]Department of Biochemistry, Adekunle Ajasin University, Akungba Akoko, Ondo State, Nigeria. mactomiwa@gmail.com

*Corresponding author: Opeyemi Iwaloye

popenapoleon@gmail.com

Preprints (www.preprints.org) | NOT PEER-REVIEWED | Posted: 20 December 2021 doi:10.20944/preprints202112.0296.v1

Scaffolds of 1, 2, 4, triazolo [1, 5-a] pyrimidin-7-amine as potential inhibitors of *Plasmodium falciparum* dihydroorotate dehydrogenase: Fragment-Based Drug Design, 2D-QSAR and DFT Calculation

Abstract

Plasmodium falciparum dihydroorotate dehydrogenase (*Pf*DODH) is one of the enzymes currently explored in the treatment of malaria. Although there is currently no clinically approved drug targeting *Pf*DODH, many of the compounds in clinical trials have [1, 2, 4,] triazolo [1, 5-a] pyrimidin-7-amine backbone structure. This study sought to design new compounds from the fragments of known experimental inhibitors of *Pf*DODH. Nine experimental compounds retrieved from Drug Bank online were downloaded and broken into fragments using Schrodinger power shell; the fragments were recombined to generate new ligand structures using BREED algorithm. The new compounds were docked with *Pf*DODH crystal structure, after which the compounds were filtered with extensive drug-likeness and toxicity parameters. A 2D-QSAR model was built using the multiple linear regression method and externally validated. The compounds electronic behaviours were studied using DFT calculations. Structural investigation of the six designed compounds, which had lower binding energies than the standard inhibitors, showed that five of them had [1, 2, 4,] triazolo [1, 5-a] pyrimidin-7-amine moieties and interacted with essential residues at the *Pf*DODH binding site. In addition to their drug-like and pharmacokinetic properties, they also showed minimal toxicities. The externally validated 2D-QSAR model with R^2 and Q^2 values of 0.6852 and 0.6691, confirmed the inhibitory prowess of these compounds against *Pf*DODH. The DFT calculations showed regions of the molecules prone to electrophilic and nucleophilic attack. The current study thus provides insight into the development of a new set of potent *Pf*DODH inhibitors.

Keywords: *Plasmodium falciparum* dihydroorotate dehydrogenase, fragment-based drug design, 2D-QSAR, DFT calculation, Lead optimization, Induced Fit docking

 doi:10.20944/preprints202112.0296.v1

Introduction

With estimated mortality of at least 400,000 each year, malaria is arguably one of the most devastating parasitic infectious diseases [1]. Malaria is an endo-parasitic disease endemic to developing countries in Asia, Sub-Saharan Africa and South America [2]. Sub-Saharan Africa is the worst hit by malaria, causing approximately 438,000 deaths in 2015, with about 90% of the cases occurring in children below the age of five (5) [3]. The comorbidities and mortalities associated with malaria have negatively impacted Africa's socio-economic development [2]. Several approaches, including control of disease vector (female anopheles mosquito), vaccines and chemotherapy, have been explored to combat malaria. In spite of the successes recorded by some of these strategies, certain drawbacks such as drug resistance, insecticide resistance, and low efficacy have resulted in the persistence of malaria [4].

Chemotherapy is undoubtedly one of the major successfully used approaches to combat malaria. Different chemotherapeutic drugs such as quinine, chloroquine, and pyrimethamine/sulfadoxine, artemisinin combination therapies (ACTs) have been developed over the years to eliminate infectious malaria causing plasmodium parasites. *Plasmodium malariae*, *Plasmodium knowelsi*, *Plasmodium ovalae*, *Plasmodium vivax* and *Plasmodium falciparum* are the five malaria causing pathogens and have been a subject of intense research studies of the years. Currently, the most effective chemotherapeutic agents available for the treatment of malaria are ACTs which have shown an outstanding 90% efficacy in uncomplicated malaria treatment [5,6]. However, the past few decades has seen the development of drug resistant *Plasmodium falciparum* strains that are insensitive to ACTs and other malaria drugs, resulting in global resurgence of malaria [7–9]. The current surge in the prognosis of malaria has spurred intensive research on identifying novel therapeutic regimens as alternatives for the current antimalarial drugs. Recent studies have focused on identifying drugs that target proteins involved in metabolic pathways such as heme degradation, fatty acid metabolism, nucleic acid synthesis and oxidative stress [10,11]. One of the novel prime drug targets in malaria is dihydroorotate dehydrogenase –a key enzyme in the denovo synthesis of pyrimidine nucleotide in plasmodium.

Dihydroorotate dehydrogenase (DHODH) is a flavin mononucleotide dependent enzyme that catalyzes the conversion of dihydroorotate to orotic acid, the fourth step in the pyrimidine de novo synthesis pathway. While there are two sub-cellular locations of DHODH (cytoplasm and

Preprints (www.preprints.org) | NOT PEER-REVIEWED | Posted: 20 December 2021 doi:10.20944/preprints202112.0296.v1

mitochondria), plasmodium species only have the mitochondria type II DHODH enzyme, which is localized in the inner mitochondria membrane [12]. DHODH has become an attractive target in malaria treatment because of its essential role in the de novo synthesis of pyrimidine and its profound druggable tendencies which exceeds that of other proteins in the pathway [13]. Plasmodium species cannot synthesize pyrimidine nucleotide through the salvage pathway –the alternative pathway for pyrimidine synthesis, thus blocking the de novo synthesis pathway results in the death of the parasite. Moreover, the *Plasmodium falciparum* dihydroorotate dehydrogenase (*Pf*DODH) possesses a unique binding site different from human DHODH which allows for increased drug specificity [13]. So far, different selective inhibitors of *Pf*DODH have been designed and are currently in different stages of clinical trials, but none has been approved by FDA as standard antimalarial drug. Perhaps one of the best successes recorded so far in the development of *Pf*DODH inhibitor as antimalarial drug is the design and synthesis of triazolopyrimidine-based DHODH inhibitor. Triazolopyrimidines are pure isoteric analogs with a profound influence on protein biosynthesis.

Philips et al. conducted high throughput screening of a library of 220,000 compounds and identified DSM1, a compound consisting of 5-methyl,2-napthyl substituted pyrimidine-7-amine structure with significant DHODH inhibitor activity under *in vitro* [13]. Preclinical studies on DSM1, however, showed no *in vivo* efficacy which spurred research to develop drugs with better efficacy under *in vivo* conditions [4]. Subsequent lead optimization studies by replacement of napthyl with phenyl group, and addition of fluorine led to the identification of other 7-aryl amino triazolopyrimidine derivatives such as DSM74, DSM190, DSM-330, DSM-331 and DSM338 which showed moderate *in vivo* activity [14,15]. Philips et al. later developed DSM265 consisting of a triazolopyrimidine scaffold with a pentaflurosurafanyl (SF_5) group which showed profound DHODH inhibition efficacy and is currently in phase II clinical trials –making it the only SF_5 containing compound in clinical trials [13,15]. Lead compounds like P218, Genz-669178 and DSM 267 among others have also shown promising prospects and are currently undergoing clinical assessments [2,4,16]. Despite the significant prospects of these compounds, recent studies have shown the development of resistance by *P. falciparum* to some of these lead compounds [16]. Furthermore, there are concerns regarding the pharmacokinetic properties of some of the developed DHODH inhibitors [4,17]. Although DSM 265 was reported to have good pharmacokinetic properties, specific related adverse effects such as headache and gastrointestinal

Preprints (www.preprints.org) | NOT PEER-REVIEWED | Posted: 20 December 2021 doi:10.20944/preprints202112.0296.v1

symptoms were reported during human trials [18]. In an attempt to mitigate the challenge faced by current DHODH inhibitors, including those with triazolopyrimidine scaffolds, fragment based drug design was adopted in the current study to design new DHODH inhibitors from triazolopyrimidine scaffold with increased efficacy, better selectivity and good pharmacokinetic properties.

Fragment based drug design (FBDD) involves the development of lead compounds from fragments with molecular masses not exceeding 350 Da [19]. FBDD has been shown to offer certain comparative advantages over high throughput virtual screening among which are high chemical diversity, identification of lead compounds with low molecular weights and improved ligand efficiency due to lead optimization [20]. In the current study, using fragments based drug design techniques novel inhibitors of *Pf*DODH were designed. Molecular docking virtual screening and QSAR modeling was performed to assess the efficacy of the designed compounds.

Materials and methods

Protein preparation

The authors picked PDB ID: 6VTN as the protein crystal structure of *Plasmodium falciparum* dihydroorotate dehydrogenase (*Pf*DODH) for this *in silico* study. The protein is non-covalently bound with DSM557, a promising inhibitor currently experimented in clinical trials. 6VTN has resolution of 2.25 Å, R-Value Free: 0.219, R-Value Work**:** 0.202 and R-Value Observed of 0.204. Further investigation showed that 6VTN has a single chain (Chain A) with 401 sequence length and no mutation. This protein (PDB ID: 6VTN) was downloaded by typing "6VTN" on Schrodinger suite (version 2020-3) using protein preparation wizard panel. The Schrodinger suite automatically retrieved the protein from the protein data bank repository (http;//www.rcsb.org) and uploaded the protein crystal structure into the workspace of Maestro (version 12.5). Subsequently, the protein was prepared using the protein preparation wizard. Protein preparation is a crucial stage in molecular docking because it helps to correct errors that may be present in the crystal structure of the protein. With this in mind, the following were performed during the preparation of the protein: missing hydrogen was added, bond orders were assigned, the hydroxyl, ASN, GLN and HIS were optimized, and finally restrained minimization was carried out using a well authenticated force field (OPLS3e).

Preprints (www.preprints.org) | NOT PEER-REVIEWED | Posted: 20 December 2021 doi:10.20944/preprints202112.0296.v1

Generation of compounds library for fragment based drug design and compounds preparation

Nine experimental compounds that have been used in trials studying the prevention and treatment of Malaria targeting *Pf*DODH were retrieved from DrugBank database (https://www.drugbank.ca/) [21]. The DrugBank database is a unique bioinformatics and cheminformatics resource that combines detailed drug (i.e. chemical, pharmacological and pharmaceutical) data with comprehensive drug targets (i.e. sequence, structure, and pathway) information. The compounds include DSM74 (5-Methyl-N-[4-(trifluoromethyl)phenyl][1,2,4]triazolo[1,5-a]pyrimidin-7-amine), KAF156 (ganaplacide), DSM338 (N-[3,5-Difluoro-4-(Trifluoromethyl)phenyl]-5-Methyl-2 (Trifluoromethyl)[1,2,4]triazolo[1,5-A]pyrimidin-7-Amine), DSM190 (N-[3,5-Difluoro-4-(trifluoromethyl)phenyl]-5-methyl-[1,2,4]triazolo[1,5-a]pyrimidin-7-amine), DSM265 (2-(1,1-difluoroethyl)-5-methyl-N-[4-(pentafluoro-lambda6-sulfanyl)phenyl]-[1,2,4]triazolo[1,5-a]pyrimidin-7-amine), DSM330 (2-(1,1-Difluoroethyl)-N-[3-fluoro-4-(trifluoromethyl)phenyl]-5-methyl-[1,2,4]triazolo[1,5-a]pyrimidin-7-amine), DSM331 (2-(1,1-Difluoroethyl)-N-[3,5-difluoro-4-(trifluoromethyl)phenyl]-5-methyl[1,2,4]triazolo[1,5-a]pyrimidin-7-amine), DSM276 (2-(1,1-Difluoroethyl)-5-Methyl-N-[4-(Trifluoromethyl)phenyl][1,2,4]triazolo[1,5-A]pyrimidin-7-Amine) and p218 (3-(2-{3-[(2,4-Diamino-6-Ethylpyrimidin-5-Yl)oxy]propoxy}phenyl)propanoic Acid). The two dimensional structure of the aforementioned compounds were download from PubChem database (https://pubchem.ncbi.nlm.nih.gov/), and uploaded into the workspace of Maestro for preparation by LigPrep module.

Generation of fragments

The nine (9) prepared compounds were converted into fragment using the command line "**run fragment.molecule.py**" on Schrodinger power shell. A total of 210 fragmented molecules were computed, and the fragments were docked into the active site of the protein using extra precision (XP) glide algorithm.

Breed ligand creation and molecular docking

About 90 fragments had a docking score of -6.00 kcal/mol and above, and these fragments were recombined to generate new ligand structures using BREED algorithm [22]. The BREED

Preprints (www.preprints.org) | NOT PEER-REVIEWED | Posted: 20 December 2021 doi:10.20944/preprints202112.0296.v1

algorithm works using the following principle: "A group from one ligand can be swapped with a group from another ligand if the bond to the group in the first ligand overlaps with the bond to the group in the second ligand. The bonds are considered to overlap if the angle between the two bonds is less than a specified maximum value and the atoms at each end of the bond in the first ligand are no further away from the corresponding atoms in the second ligand than a specified maximum value." The module BREED generated 120 new set of designed compounds. The generated compounds were docked with *Pf*DODH (using glide XP docking algorithm) to calculate their binding energies with the protein. Fifty top-scoring compounds (in term of binding energy) were regarded as hit compounds.

Binding free energy and flexible docking score determination

The binding free energy of the compounds were calculated by uploading the protein-ligand complex files on PRIME MM-GBSA module. The prime MMGBSA calculates the free energy difference between the minimized protein-ligand complex and the unbound protein and ligand based on the equation below:

E minimized complex = E minimized protein – E minimized ligand

The induced fit docking (IFD) methodology was implemented to optimize the energy released during binding of the compounds with flexible amino acid residues at the active site of *Pf*DODH.

Filtering of the hit compounds using PAIN and other parameters

The chosen 50 top scoring compounds were further filtered using PAIN, BRENK, Lipinski's rule of five (RO5), Veber rule, solubility and Gastrointestinal (GI) absorption.

Determination of pharmacokinetic and toxicity properties of the compounds

The compounds possibility of interacting with principal isoenzymes of cytochrome p450 were determined using SwissADME online server (http://www.swissadme.ch/) [23], and their toxicities were also evaluated by PROTOX-II webserver [24].

Density functional theory (DFT) calculation

Using the Schrödinger Materials science (version 3.9) that accommodates Jaguar fast engine, the compounds reactivity which includes frontier molecular orbitals (FMOs) and molecular

Preprints (www.preprints.org) | NOT PEER-REVIEWED | Posted: 20 December 2021 doi:10.20944/preprints202112.0296.v1

electrostatic potential (MEP) was estimated using 6-31G** as basic set and Becke's three-parameter exchange potential and Lee-Yang-Parr correlation (B3LYP) as level of functional theory.

Construction of 2D QSAR model and its validation

Datasets comprising seventy-eight (78) *Pf*DODH inhibitors from experimental assays were obtained from CHEMBL database web server along their logarithmic IC50 value [25]. The compounds were minimized by single point energy calculation on Jaguar using 6-31G** as basic set and Becke's three (B3LYP) as level of functional theory. The compounds were exported to Canvas software (version 3.5) to generate 2D descriptors and the fingerprints of the 78 experimental compounds. The highly correlated descriptors were deleted using feature selection option on Canvas. The multiple linear regression method used low correlated 2D descriptors of the dataset to construct the QSAR model by randomly splitting the training and test set into 58 and 20. The constructed QSAR model was validated using the Xternal validation plus tool designed by Roy et al. [26].

Results and Discussion

P. falciparum has become one of the primary cause of health challenges in the world, especially in malarial epidemic regions such as sub-Saharan Africa, Asia and Latin America, whose prevalence is on the rise with each passing year [2]. The development of drug resistance by *P. falciparum* parasite constitutes one of the major challenges in malaria control which has led to the increase in malarial-related death worldwide [4]. New strategies have been developed to arrest the challenges of drug-resistance *P. falciparum,* and one such approach lies in the design and development of chemical compounds that can inhibit *Pf*DODH, a prime target in the treatment of malaria [12].

Preliminary screening of the fragment-based compounds

In this study, nine of the experimental compounds that have showed the most promising therapeutics against *Pf*DODH were retrieved and assembled. Inspection of the chemical structure of these compounds (especially the DSMs) showed that they contain methyl- [1, 2, 4,] triazolo

Preprints (www.preprints.org) | NOT PEER-REVIEWED | Posted: 20 December 2021 doi:10.20944/preprints202112.0296.v1

[1, 5-a] pyrimidine as their backbone structure with multiple fluorine atoms attached to its phenyl ring (Figure 1).

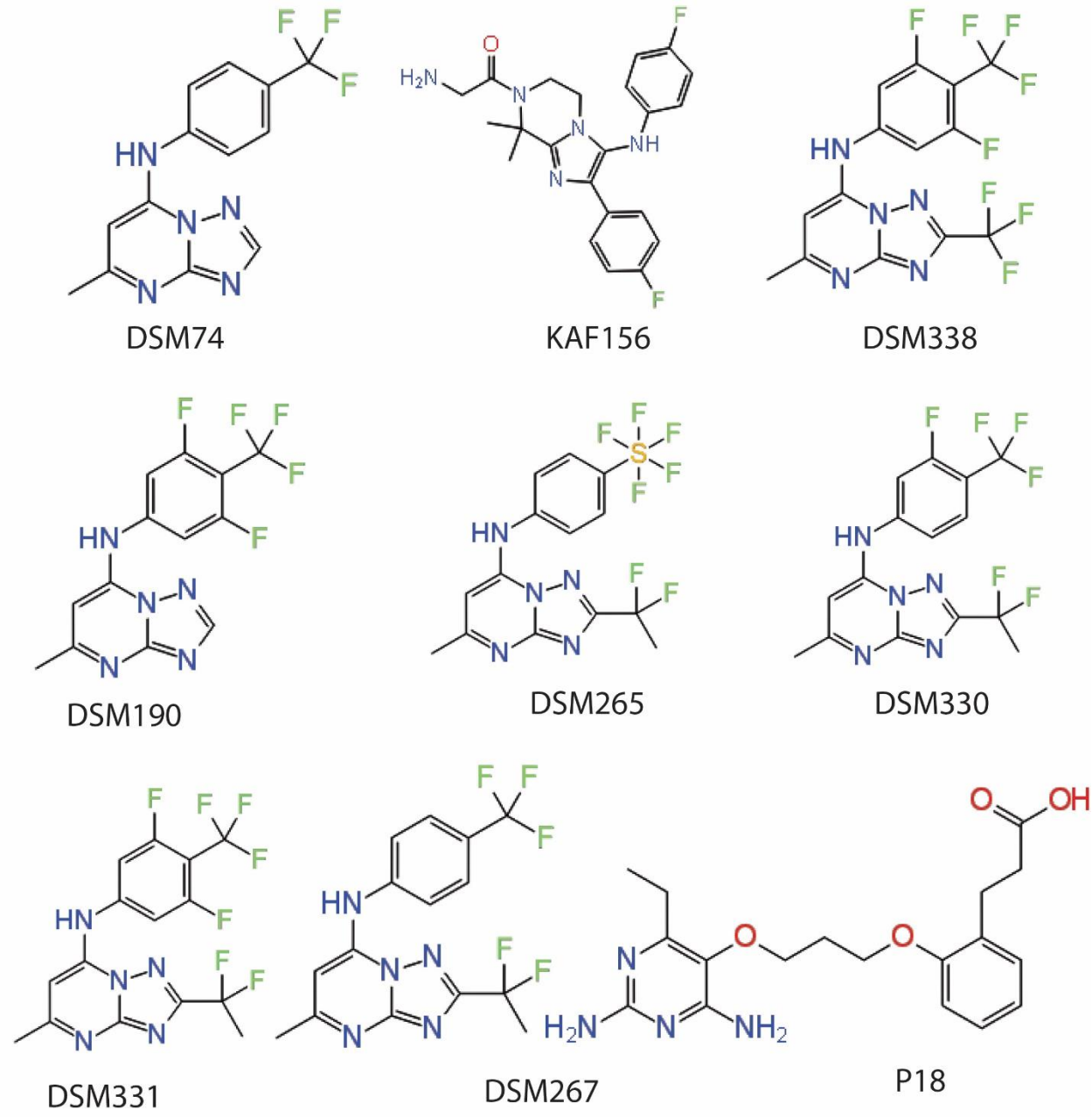

Figure 1: 2D structure of the DHODH standard inhibitors used for designing a new set of drug-like molecules.

Preprints (www.preprints.org) | NOT PEER-REVIEWED | Posted: 20 December 2021 doi:10.20944/preprints202112.0296.v1

The compounds were broken into fragments and redesigned using the breed ligand creation algorithm, followed by molecular docking simulation. This research chose 50 compounds as the most preferred compounds because they had docking score of -6.00 kcal/mol and more. However, these compounds were further filtered using binding free energy, GI absorption, PAIN, BRENK, Lipinski's rule of five (RO5), Veber rule, P-gp substrate and solubility (Log S). Pan-assay interference compounds (PAINS) are chemical compounds that often give false positive results in high-throughput screening [27]. PAINS tend to react nonspecifically with numerous biological targets rather than specifically affecting one desired target [28]. BRENK filters unwanted functionality due to potential toxicity reasons or unfavorable pharmacokinetics [29]. On the other hand, RO5 filters compounds based on oral bioavailability [30], whereas Veber rule determines the drug-likeness of compounds based on rotatable bound count (<= 100) and polar surface area (PSA) (<= 140). Solubility determines the absorption and bioavailability of compounds after oral dosing, which correlates with GI absorption. P-glycoprotein is a cell membrane protein that pump foreign substance out of cell, and compounds that are substrate of P-glycoprotein are eliminated from the cells (Table S1). Six of the newly designed compounds (YME002, YME003, YME004, YME006, YME007 and YME009) with clean ADME profiles and favorable docking score were selected as the hits compounds. In the same vein, the same set of parameters were used to filter the experimental compounds from which the hit compounds were designed (Table S2), and the two most favorable compounds (DMS330 and DSM74) in term of binding energy (docking score) with *Pf*DODH were used as means of comparison with the hit compounds.

Structural description of the hit compounds

Structural investigation of the newly designed top scoring compounds showed that the compounds (with the exception of YME002) all had [1, 2, 4,] triazolo [1, 5-a] pyrimidin-7-amine moiety as backbone structure. Structurally, YME002, contains two phenyl rings connected together via nitrogen trihydride. Attached to the first phenyl ring of YME002 at position 13 are three atoms of fluorine. The phenyl ring and 2-aminoacetaldehyde of YME002 are attached to the compound's backbone structure at position 7 and 10. YME003, another compound with structure different from YME002 but similar to other compounds, housed [1, 2, 4,] triazolo [1, 5-a] pyrimidin-7-amine, and contains a single fluorine atom attached to its benzene ring. The

Preprints (www.preprints.org) | NOT PEER-REVIEWED | Posted: 20 December 2021 doi:10.20944/preprints202112.0296.v1

backbone structure of YME004 connect to its phenyl ring via nitrogen trihydride, and the phenyl ring housed 4 fluorine atoms and a methyl group. YME006 contains [1, 2, 4,] triazolo [1, 5-a] pyrimidin-7-amine moiety as backbone structure connects with a phenyl ring that housed other functional groups. The other newly designed compounds (YME007 and YME009) are structurally similar. Whereas the backbone of YME007 is connected to carbonyl oxygen, the backbone structure of YME009 is structurally connected to 2-aminoacetaldehyde.

Molecular docking and post-docking analysis

The interpretation of the molecular docking study showed that the six newly designed compounds had binding affinity with *Pf*DODH, way better than the reference compounds (Table 1). YME002, YME003, YME004, YME006, YME007 and YME009 had binding energy of -10.740 kcal/mol, -9.672 kcal/mol. -9.450 kcal/mol, -8.041 kcal/mol, -7.906 kcal/mol and -7.8 kcal/mol, respectively. Also, DSM330 and DSM74 had binding energy of -7.556 kcal/mol and -7.459 kcal/mol. The favorable docking score by the six compounds upon binding to *Pf*DODH when compared with the standard inhibitors can be attributed to their structural diversity. The molecular docking study was further validated by calculating the binding free energy of the protein-ligand complexes.

Table 1: comprehensive molecular docking studies and inhibitory potential of the newly designed compounds and standard inhibitors against *Pf*DODH

Name	**Docking score**	**Binding free energy**	**IFD**	**H-bond/pi-pi interaction**	**Hydrophobic interactions**	**pIC50**
YME002	-10.740	-40.167	-837.41	VAL532, **PHE188**	TYR168, PHE171, LEU172, MET536, CYS175, LEU176, VAL532, LEU531, CYS184, PHE185, PHE227, LEU187, PHE188, LEU191	-5.79
YME003	-9.672	-35.976	-835.07	ARG265, GLYS181, **HIE185**	LEU191, TYR168, PHE188, PHE171, LEU171, LEU187, CYS175, CYS184, LEU176, CYS184, ILE263, ILE272, LEU531, PHE227, VAL532, MET536	-6.96
YME004	-9.450	-31.862	-831.02	ARG265	TYR168, PHE171, LEU172, MET536, CYS175, VAL532, ILE263, TYR528, CYS184, PHE227, LEU187,	6.70

Preprints (www.preprints.org) | NOT PEER-REVIEWED | Posted: 20 December 2021 doi:10.20944/preprints202112.0296.v1

					PHE188, LEU191, LEU197	
YME006	-8.041	-33.338	-830.93	CYS184, **HIE185***	MET536, TYR168, PHE171, LEU191, LEU172, CYS175, ILE263, ILE262, TYR528, LEU531, PHE227, VAL532	6.41
YME007	-7.906	-33.605	-826.09	CYS184, PHE188	LEU172, PHE171, LEU191, TYR168, PHE188, LEU187, CYS184, ILE262, ILE263, TYR528, PHE227, LEU531, VAL532, MET536	6.82
YME009	-7.8	-10.953	-822.84	ARG265, GLY181, HIE185	TYR168, PHE171, LEU172, CYS175, LEU176, ILE272, ILE263, CYS184, PHE227, LEU531, VAL532, LEU187, PHE188, LEU191, MET536	7.02
DSM330*	-7.556	-35.97	-830.55	GLY181	ILE272, TYR528, LEU53, PHE227, LEU240, VAL532, MET536, ILE263, CYS184, LEU176, CYS175, LEU187, PHE188, LEU172, PHE171, LEU191, TYR168	6.75
DSM74*	-7.459	-38.92	-827.61	PHE118, PHE171	TYR168, LEU191, PHE171, LEU172, PHE188, LEU187, CYS175, LEU176, CYS184, LEU531, VAL531, MET536	6.54

The binding free energy is one of the most reliable methods of validating docking score [31,32], and the results showed that all the investigated compounds had favorable binding free energy which denote accuracy of docking score results. During the preliminary screening of the top 50 newly designed compounds from fragments of known inhibitors, some of the compounds had positive value for binding free energy (Table S1). It denotes that the docking score was false. However, these compounds were filtered out before the hit compounds were picked. During investigation of the interaction between the compounds and the proteins using pose viewer of Maestro, it was found that little or no intermolecular interaction exist between the compounds and amino acid residues within the active site of *Pf*DODH (see Table 1). Thus, flexible docking, a computationally expensive method was explored to further visualize the type and number of amino acid residues the compounds made contact with. Unlike the conventional docking

Preprints (www.preprints.org) | NOT PEER-REVIEWED | Posted: 20 December 2021 doi:10.20944/preprints202112.0296.v1

algorithm that do not take the geometry of the protein into consideration when docking is performed, the induce fit or flexible docking considers the rotation of the ligand and flexibility of the protein amino acid residues within the binding site [33]. The IFD results showed a more improved binding affinity between the compounds and *Pf*DODH when compared with results obtained from rigid docking. More interestingly, the decreasing order of binding affinity of the compounds with *Pf*DODH as seen in rigid docking results was also demonstrated by the results obtained from induced fit docking. YME002, YME003, YME004, YME006, YME007 and YME009 recorded IFD scores of -837.41 kcal/mol, -835.07 kcal/mol, -831.02 kcal/mol, -830.93 kcal/mol, -826.09 kcal/mol, -822.84 kcal/mol and -822.84 kcal/mol, respectively (Table 2). Unlike rigid docking, the flexible docking score of DSM330 and DSM74 were way higher than some of the newly designed compounds (Table 2). The increased intermolecular interactions of the standard inhibitors with the residues of *Pf*DODH may be responsible for the favourable binding energy.

Inhibition of *Pf*DODH by the compounds via interacting amino acid residues

In accordance with report by Vikram and Mishra [34], the amino acid located within the binding site of the *Pf*DODH are MET536, GLY535, VAL532, LEU531, TYR528, ARG265, ILE263, PHE227, LEU189, PHE188, HIE185, CYS175, LEU172, and PHE171. The putative binding site residues was also validated by another literature [35]. These residues play an important catalytic role in the inhibition of *Pf*DODH by making intermolecular contact with small molecular weight compounds [35]. In brief, the inhibitor binding site of *Pf*DODH can be categorically classified into two pockets. The first is the hydrogen binding site consisting of residues ARG265 and CYS175, and the second is the hydrophobic cavity formed by the helices αA and αB [36].

Preprints (www.preprints.org) | NOT PEER-REVIEWED | Posted: 20 December 2021 doi:10.20944/preprints202112.0296.v1

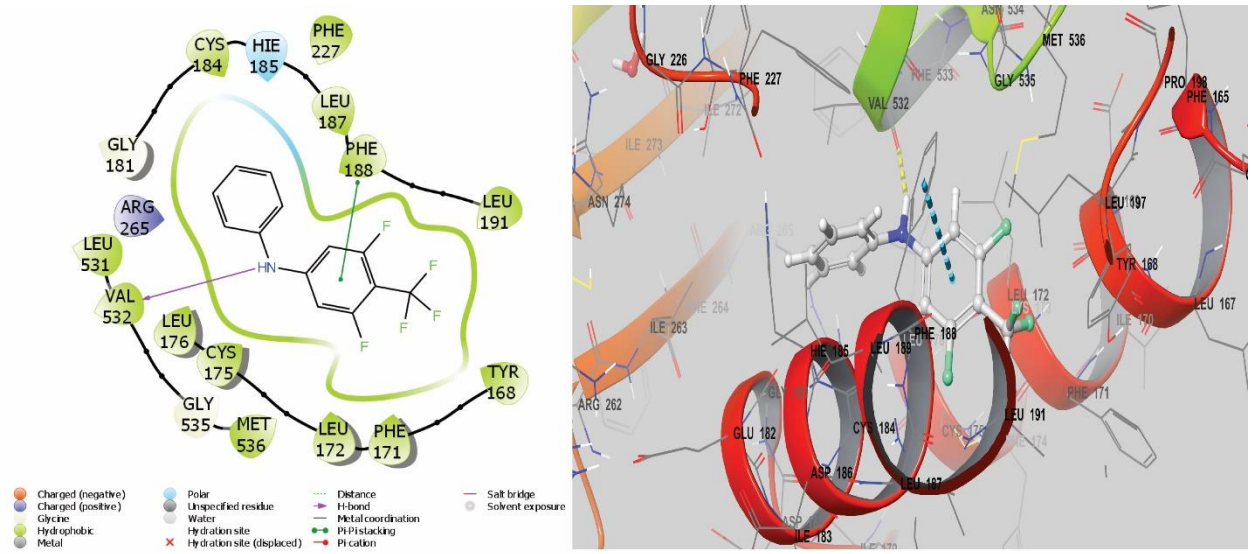

Figure 2: 2D and 3D diagram showing the intermolecular interactions between YME002 and amino acid residues of *Pf*DODH

Therefore, it is not surprising that the binding pockets of *Pf*DODH are occupied by hydrophobic amino acid residues (Figure 2 -6). In addition to the H-bond contact with ARG265 and CYS175, Deng et al. [37] showed that inhibitors can form another type of non-covalent intermolecular interaction known as pi-pi stacking with GLY181, GLU182 and HIE185. The mapping of the interactions between the newly designed inhibitors and *Pf*DODH (Table 1, Figure 2-7) highlighted the importance of hydrogen bond interactions between the compounds and VAL532, ARG265, GLYS181, CYS184 and PHE188; and the importance of pi-pi interactions between the compounds and PHE188 and HIE185. This type of interactions were also demonstrated by Hoelz et al., [36] who described the structural basis approach in the development of new inhibitors against *Pf*DODH.

Preprints (www.preprints.org) | NOT PEER-REVIEWED | Posted: 20 December 2021 doi:10.20944/preprints202112.0296.v1

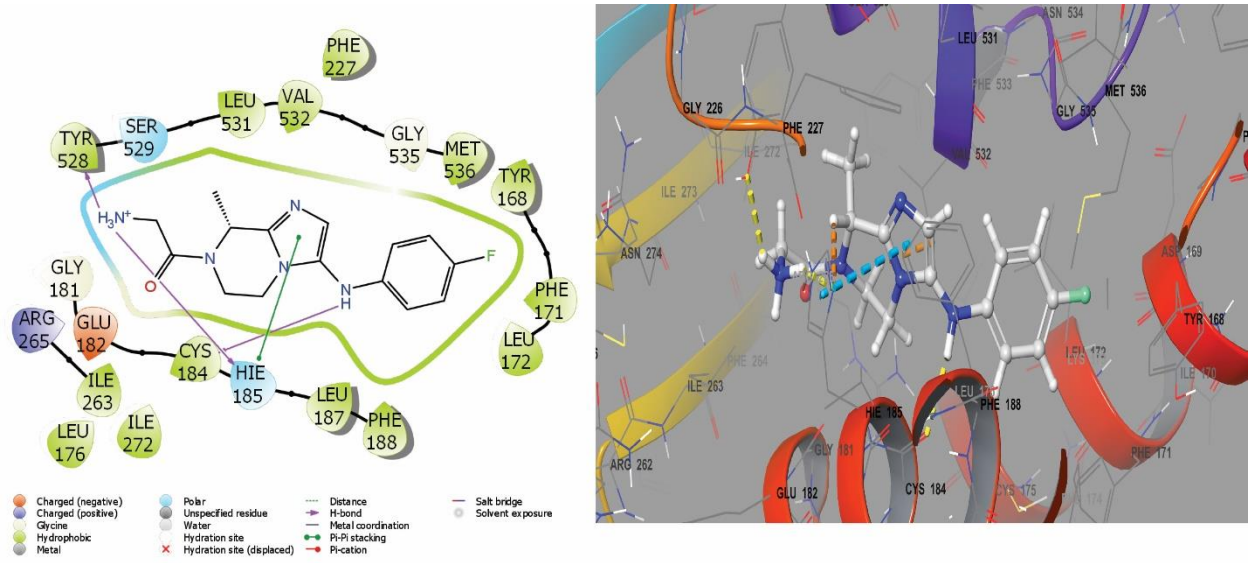

Figure 3: 2D and 3D diagram showing the intermolecular interactions between YME003 and amino acid residues of *Pf*DODH

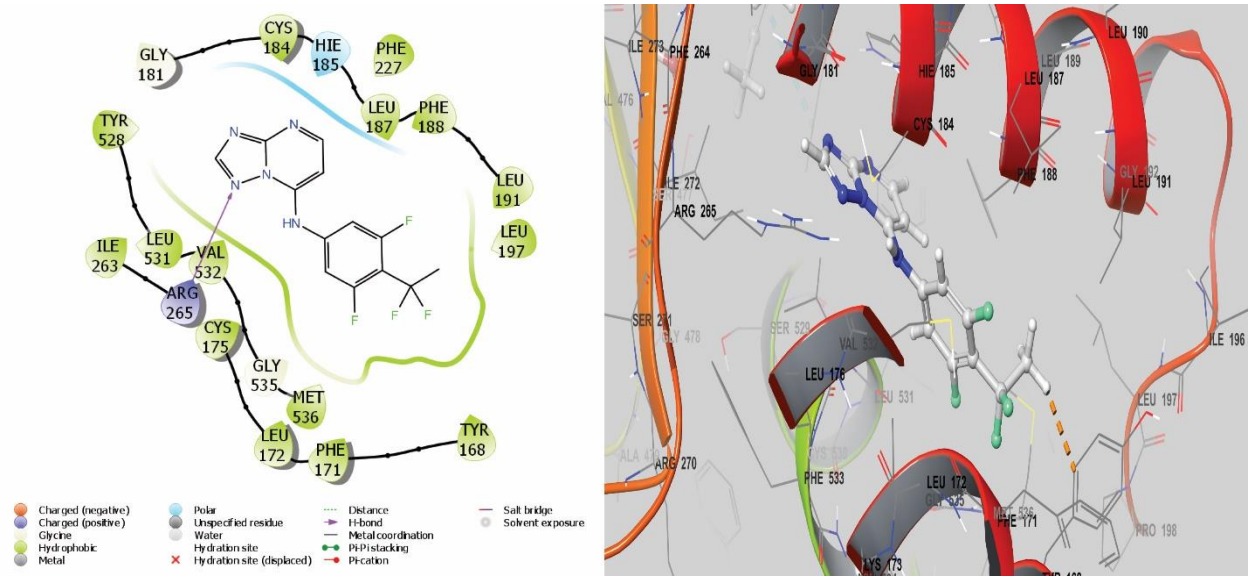

Figure 4: 2D and 3D diagram showing the intermolecular interactions between YME004 and amino acid residues of *Pf*DODH

Preprints (www.preprints.org) | NOT PEER-REVIEWED | Posted: 20 December 2021 doi:10.20944/preprints202112.0296.v1

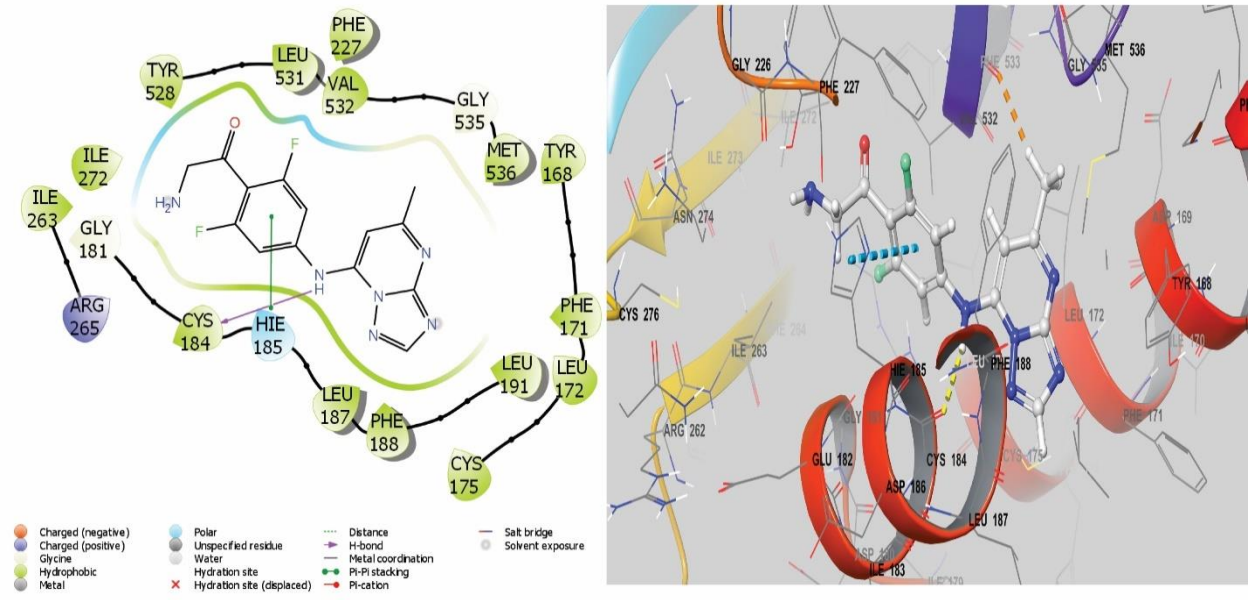

Figure 5: 2D and 3D diagram showing the intermolecular interactions between YME006 and amino acid residues of *Pf*DODH

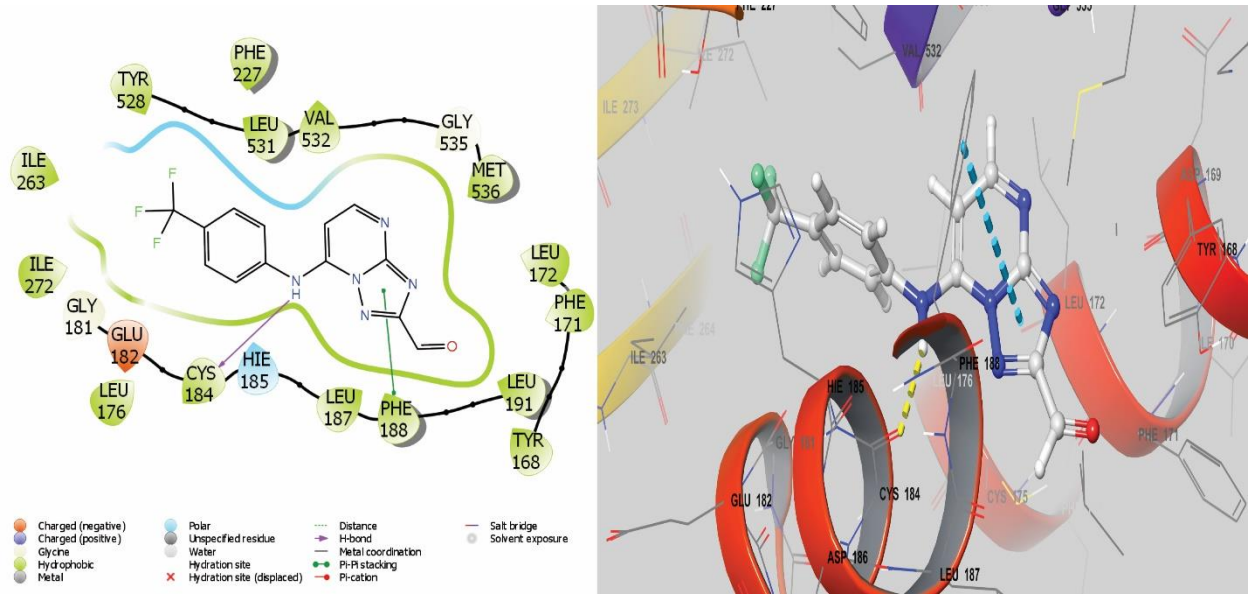

Figure 6: 2D and 3D diagram showing the intermolecular interactions between YME007 and amino acid residues of *Pf*DODH

Preprints (www.preprints.org) | NOT PEER-REVIEWED | Posted: 20 December 2021 doi:10.20944/preprints202112.0296.v1

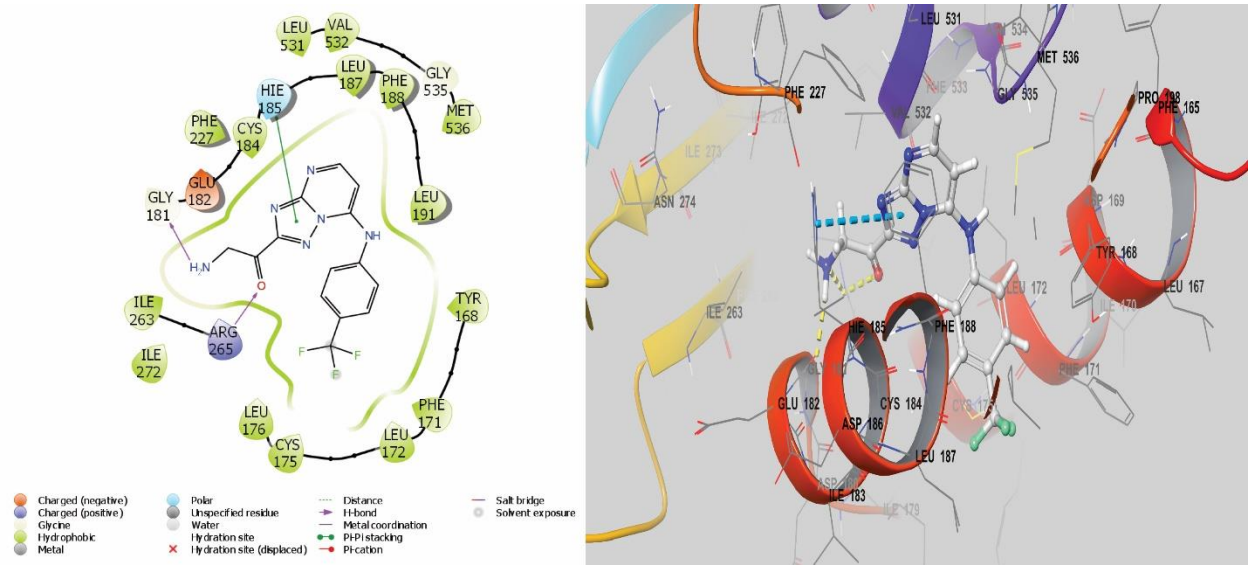

Figure 7: 2D and 3D diagram showing the intermolecular interactions between YME009 and amino acid residues of *Pf*DODH

Pharmacokinetics and toxicity properties of the newly designed compounds

The isoenzymes of cytochrome P450 are principal enzymes responsible for the biotransformation of drugs and determinant of drug interaction that can induce toxicity [38]. The isoenxymes CYP1A2, CYP2C19, CYP2C9, CYP2D6, and CYP3A4 of CYP450 were taken into consideration. The compounds including the standard inhibitors all inhibit the activity of one or more isoenymes (Table 2). However, YMEOO6, YME007 and YME009 showed the most moderate pharmacokinetics with the drug biotransformation enzymes by modulating interaction with only CYP1A2. CYP1A2 is actively involved the metabolism of cholesterol and other lipid. Its expression is induced by poly-aromatic hydrocarbons, found in cigarette; and other substrate include paracetamol and caffeine, among others [39]. In comparison with the three of the newly designed scaffold of [1, 2, 4,] triazolo [1, 5-a] pyrimidin-7-amine (YME003, YME006, YME007 and YME009), the standard inhibitors showed inhibition of CYP1A2, CYP2C19 and CYP2C9 isoenzymes, which implies that these compounds may increase through drug-drug interaction after administration of drugs that are substrates of these enzymes. Additionally, parameters such as hepatotoxicity, carcinogenicity, immunotoxicity, mutagenicity and cytoxicity were used as determinants for the compounds' toxicity. These unwanted properties affect

Preprints (www.preprints.org) | NOT PEER-REVIEWED | Posted: 20 December 2021 doi:10.20944/preprints202112.0296.v1

different cells, organs in the body either by inducing mutation or causing the dysfunction of organs or the body immune system. The results in Table 2 demonstrate that all the compounds, including the standard inhibitors, showed different levels of toxicities. All the compounds with the exception of YME002 had high tendency to cause liver toxicity. The results is not surprising because the major site of drug metabolism is the liver, and biotransformation of drugs by CYP450 isoenzymes produces metabolites, which might induce unwanted effect in the hepatocytes. Other results showed that none of the compounds are immuno-toxic or cyto-toxic. However, the compounds, including the standard inhibitors, tend to induce carcinogenicity, except YME003, YME006, YME007 and YME009. In addition to this finding, the standard inhibitors (DSM330 and DSM74) and YME002 are mutagenic substance. Overall, the compounds fell within class III and class IV of toxicity, and their lethal dose 50 (LD50) are within 275 mg/kg and 1782 mg/kg (Table 2).

Table 2: pharmacokinetic and toxicological properties of the compounds

	A	B	C	D	E	F	G	H
CYP1A2	NO	YES	YES	YES	YES	YES	YES	YES
CYP2C19	YES	NO	YES	NO	NO	NO	YES	YES
CYP2C9	NO	NO	NO	NO	NO	NO	YES	NO
CYP2D6	YES	NO	NO	NO	NO	NO	NO	NO
CYP3A4	NO	NO	NO	NO	NO	NO	NO	NO
Hepatotoxicity	Inactive	inactive	Active	Active	Active	inactive	Active	Active
Carcinogenicity	Active	Inactive	Active	inactive	Inactive	inactive	Active	Active
Immunotoxicity	Inactive	Inactive	Inactive	Inactive	Inactive	Inactive	Inactive	Inactive
Mutagenicity	Active	Inactive	Inactive	Inactive	Inactive	Inactive	Active	Active
Cytotoxicity	Inactive	Inactive	Inactive	Inactive	inactive	inactive	Inactive	Inactive
Predicted LD50 (mg/kg)	275	300	1000	300	1782	300	300mg/kg	300mg/kg
Toxicity class	III	III	IV	III	IV	III	III	III
Prediction accuracy (%)	67.38%	67.38%	54.26	54.26	67.38	67.38	54.26	67.38

A = YME002, B = YME003, C = YME004, D = YME006, E = YME007, F = YME009

Frontier molecular orbitals and global reactivity descriptors

The frontier molecular orbitals (FMOs) comprising the highest occupied molecular orbital (HOMO) and lowest unoccupied molecular orbital (LUMO) are utilized in theoretical chemistry to understand the molecular properties and reactivity of organic compounds [40]. In brief,

Preprints (www.preprints.org) | NOT PEER-REVIEWED | Posted: 20 December 2021 doi:10.20944/preprints202112.0296.v1

HOMO investigates the electron donating site of a chemical compound, and LUMO symbolizes the atomic site of a compound prone to accepting electron [41,42]. These energies are the most important orbitals that determine chemical stability of compounds [43]. The HOMO/LUMO together with the MEP were computed by DFT of Jaguar fast engine (using 6-31G** as basic set and B3LYP as level of functional theory), and the diagrammatic representation of the HOMO/LOMO region of the 6 newly designed compounds is given in Figure 8. The region of the compounds with red color indicate negative charges, and the blue color denote area with positive charge. For YME002, the only ligand among the newly designed compound without [1, 2, 4,] triazolo [1, 5-a] pyrimidin-7-amine moieties, had the HOMO centralized across its two phenyl ring, and LUMO occupied the C-C and C=C bonds of its first phenyl ring, and sit on the carbon atoms of its other benzene structure. The other 5 compounds with the same backbone structure as the standard inhibitors had their HOMO and LUMO cloud centralized majorly on the [1, 2, 4,] triazolo [1, 5-a] pyrimidin-7-amine moieties. The energy band gap (eV), computed by finding the difference between a compound HOMO and its LUMO ($HOMO_{compound\ X}$ - $LUMO_{compound\ X}$), helps to determine the chemical reactivity and kinetic stability of the compounds. In simple term, a compound with small energy gap is more polarizable and often associated with high reactivity but low kinetic stability. Based on the data provided of the energy gap of compounds in Table 3, the reactivity order of the newly designed compounds are YME002 > YME007 > YME004 > YME009 > YME006 > YME003. Based on this observation, YME002 is the most chemically hard molecule among the compounds designed from fragments, and the YME003 is the most chemically reactive compounds. It is possible that the absence of [1, 2, 4,] triazolo [1, 5-a] pyrimidin-7-amine moieties in the backbone structure of YME002 is responsible for its chemical inertness. The parameters that heavily relied on the HOMO and LUMO energies are given in Table 3. They are the global descriptors and they include, ionization potential (IP), electron affinity (EA), chemical hardness (η), chemical softness (ζ), electronegativity (χ), chemical potential (μ) and electrophilicity (ω). The following equation can used to define the global descriptors:

Ionization potential (IP) = $-E_{HOMO}$

Electron affinity (EA) = $-E_{LUMO}$

Chemical hardness (η) = $(I - A)/2$

Chemical softness (ζ) = $1/\eta$, $\chi = (I + A)/2$

Chemical potential (μ) = $-(I + A)/2$

Electrophilicity (ω) = $\mu^2/2\eta$.

Preprints (www.preprints.org) | NOT PEER-REVIEWED | Posted: 20 December 2021 doi:10.20944/preprints202112.0296.v1

Table 3: DFT calculations showing the FMOs and global descriptive parameters of the newly designed compounds

Parameters	**YME002**	**YME003**	**YME004**	**YME006**	**YME007**	**YME009**
HOMO	-0.2165	-0.3239	-0.2353	-0.2305	-0.24796	-0.23216
LUMO	-0.0229	-0.2113	-0.0753	-0.0775	-0.08569	-0.07676
Band gap	0.01936	0.1126	0.16	0.153	0.16227	0.1554
Ionization potential (I)	0.2165	0.3239	0.2353	0.2305	0.24796	0.23216
Electron affinity (A)	-0.0229	-0.2113	-0.0753	-0.0775	-0.0857	-0.07676
Chemical hardness (η)	0.5115	0.6057	0.53765	0.5387	0.5429	0.5384
Chemical softness (ζ)	1.9550	1.6511	1.8599	1.8563	1.8420	1.8574
Electronegativity (χ)	0.9771	0.7887	0.9265	0.9225	0.913	0.9232
Chemical potential (μ)	-0.9771	-0.7887	-0.9265	-0.9225	-0.913	-0.9232
Electrophilicity (ω)	0.8513	0.4743	0.7957	0.7896	0.7677	0.7915

Preprints (www.preprints.org) | NOT PEER-REVIEWED | Posted: 20 December 2021 doi:10.20944/preprints202112.0296.v1

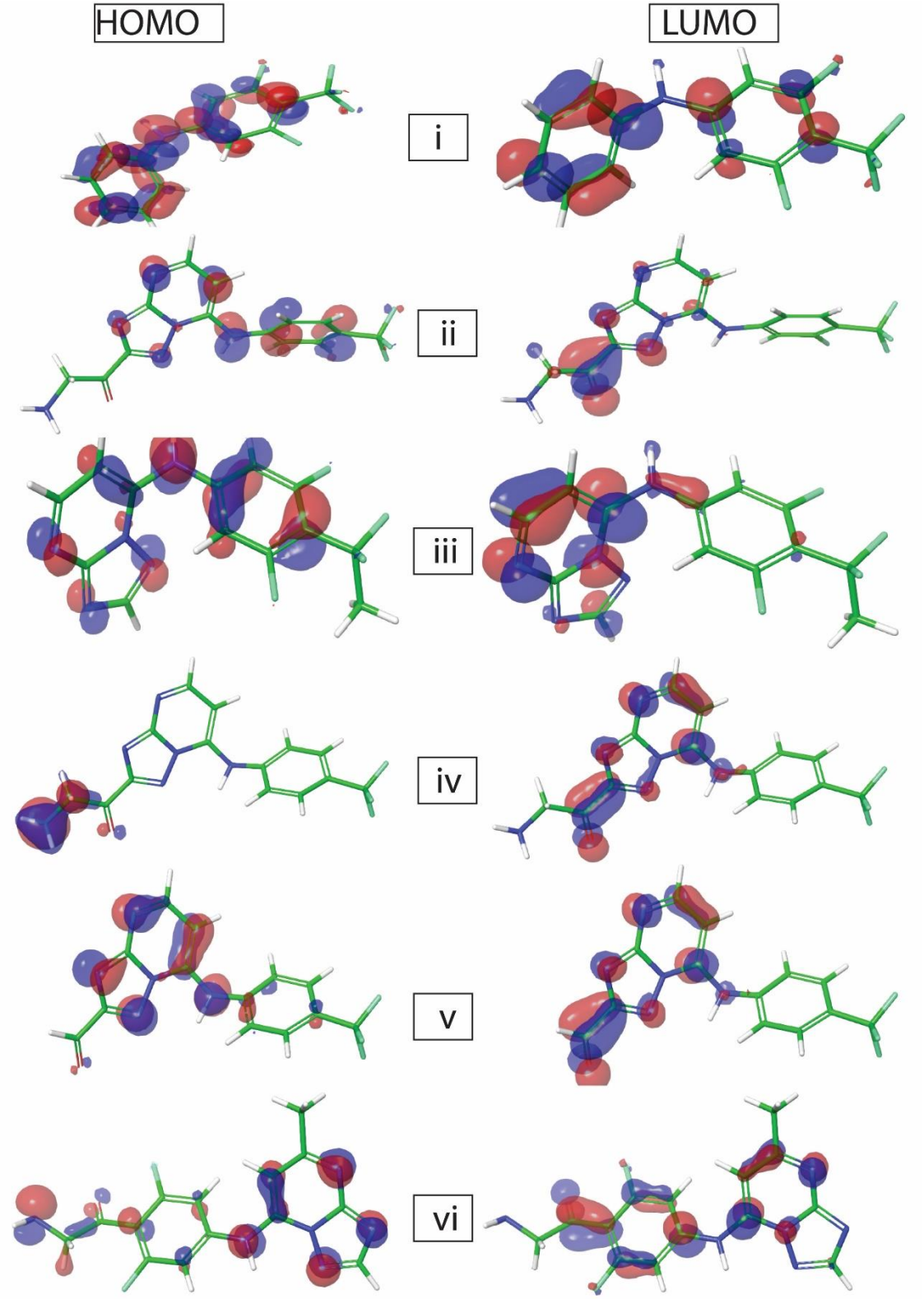

Figure 8: The a)HOMO and b) LUMO of (i) YME002 (ii) YME003 (iii) YME004 (iv) YME006 (v) YME007 (vi) YME009

 doi:10.20944/preprints202112.0296.v1

Ionization potential evaluates the chemical reactivity of molecules – high ionization potential indicate high stability and chemical inertness, and low ionization potential signifies low stability but high reactivity. Chemical hardness and softness also determine the stability and chemical reactivity of a molecule. Electron affinity explains electron accepting capacity of a compound, and electrophilicity defines the "electron-loving' or "negative-charge loving' capacity of chemical compound to accept a lone pair of electron. All the aforementioned global descriptive parameters helps to further explain the compounds ability to accept and donate electron. Overall, the newly designed compounds had significant level of reactivity (Table 3). The molecular electrostatic potential (MEP) of the compounds were calculated to understand the distribution of charges over the compound in a three-dimensional format, thereby elucidating the most electropositive (prone to nucleophilic attack) and electronegative site (prone to electrophilic attack) [44]. The MESP map of the compounds illustrated in Figure 9. These sites provide information on the atoms of the compounds that can form non-covalent interactions [45].The values of MEP at the surface of the compounds are represented by different colors, red color signifies the regions of the most electro negative electrostatic potential, blue color shows the regions of the most electro positive electrostatic potential, and the grey color represent the region with zero potential. Therefore, the electrostatic potential increases in the order red <grey < blue. The electrostatic potential contour map of the compounds as shown in Figure 9, demonstrated that the compounds have many possible sites for electrophilic (red color) and nucleophilic attack (blue color). The regions over the compounds benzene ring are neutral as represented by grey color. It is important to note that these sites give details on intermolecular interactions [44].

Preprints (www.preprints.org) | NOT PEER-REVIEWED | Posted: 20 December 2021 doi:10.20944/preprints202112.0296.v1

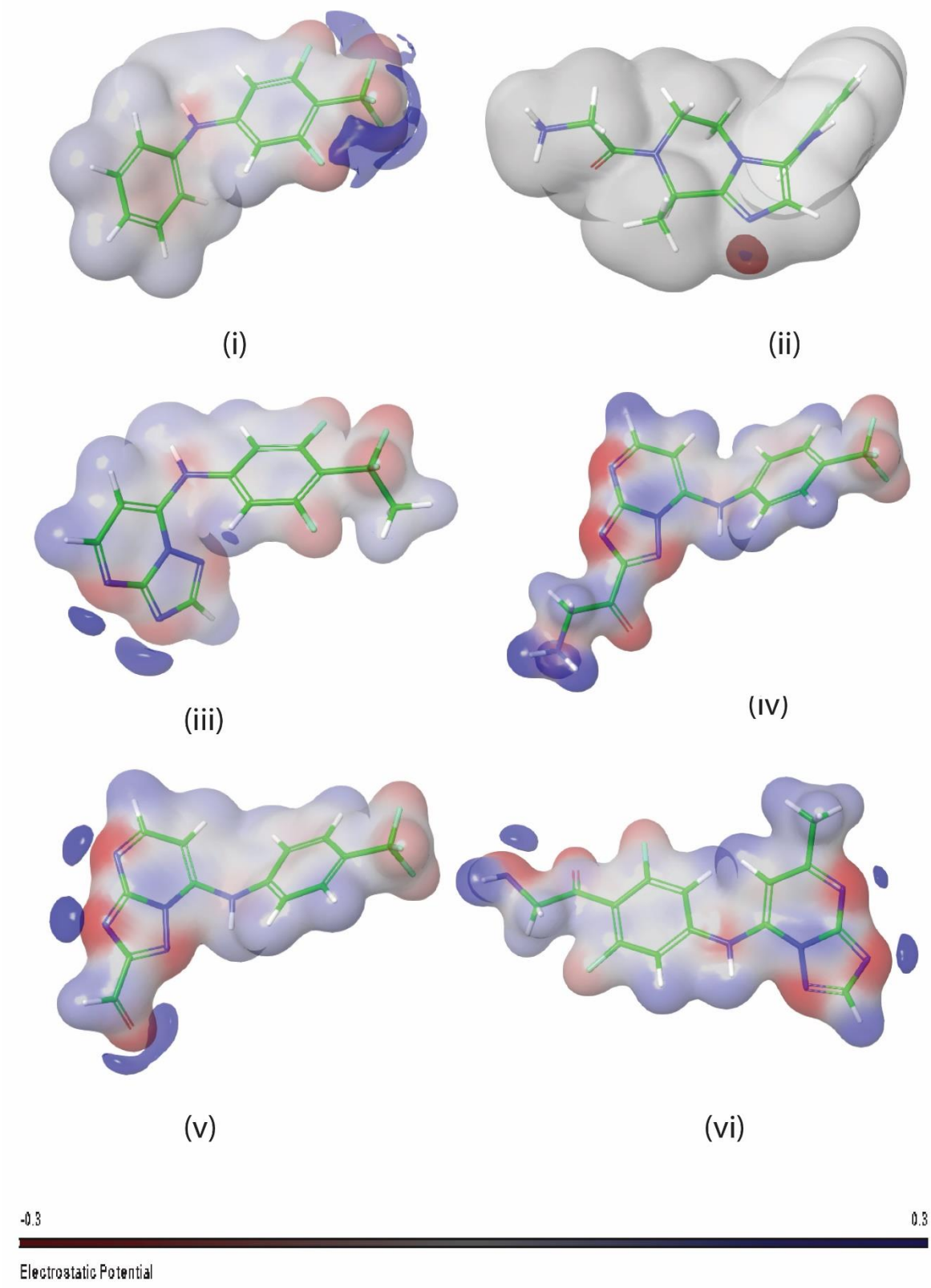

Figure 9: The molecular electrostatic potential (MEP) of (i) YME002 (ii) YME003 (iii) YME004 (iv) YME006 (v) YME007 (vi) YME009

Preprints (www.preprints.org) | NOT PEER-REVIEWED | Posted: 20 December 2021 doi:10.20944/preprints202112.0296.v1

2D QSAR modeling and external validation

The 2D QSAR model was constructed by multiple linear regression (MLR), a statistical technique that uses several descriptors to predict the outcome of a response variable (pIC50). A total of nine independent 2D descriptors were used to construct the QSAR model, and the summary of ensemble MLR model is given in Table 4. The MLR model has standard deviation of 0.6228, R^2 of 0.6852, root mean square error of 0.5814, and Q^2 of 0.66991 (Figure 10). The quantitative parameters used for generating the model using MLR are given in Table S3, and the scatter plot of the observed pIC50 against the predicted pIC50 is shown in Figure 10. The 2D QSAR model was externally validated before it was used to predict the bioactivity of the newly designed compounds against *Pf*DODH. None of the conditions is valid for the predictive model (Table 5), which shows the absence of systematic errors; therefore, other external parameters can be checked using the test set. Different classical metrics of the predictive model showed that the results fall within the acceptable value. Besides, after removing 5% of the test set data with high residuals, classical metrics also showed reliable values (Table 5). The error-based metrics denote that the values of root mean square error prediction (RMSEP), standard deviation (SD), Standard error (SE) and mean absolute error are close to zero [46]. Hence, external validation confirms the reliability and robustness of the QSAR model. The predicted bioactivities of the compounds by the 2D QSAR model confirmed the inhibitory prowess of the newly designed set of compound (Table 1), and hence validated the results obtained from the molecular docking study.

Table 4: Ensemble MLR Model Summary:

	Coefficient	**Std. Err.**	**T Variable**
Intercept	6.0894e+000	9.3222e-001	6.5321
i_canvas_RB	-4.1873e-001	8.9364e-002	4.6857
i_canvas_sOH_Cnt	7.7344e-003	1.7810e-003	4.3427
i_desc_Sum_of_topological_ distances_between_S..F	7.7344e-003	1.7810e-003	4.3427
i_ligfilter_N	-1.9648e-001	5.4329e-002	3.6165
r_desc_ALOGP3	-3.2170e-003	1.7148e-003	1.8760
r_desc_ALOGP7	4.3329e-002	9.3484e-003	4.6349
r_desc_PEOE12	-6.5512e-002	1.2143e-002	5.3950
Petitjean_2D_shape	1.9034e+000	6.9416e-001	2.7420
r_desc_Topological_charge_ index_of_order_3	4.4189e-001	1.3904e-001	3.1782

Preprints (www.preprints.org) | NOT PEER-REVIEWED | Posted: 20 December 2021 doi:10.20944/preprints202112.0296.v1

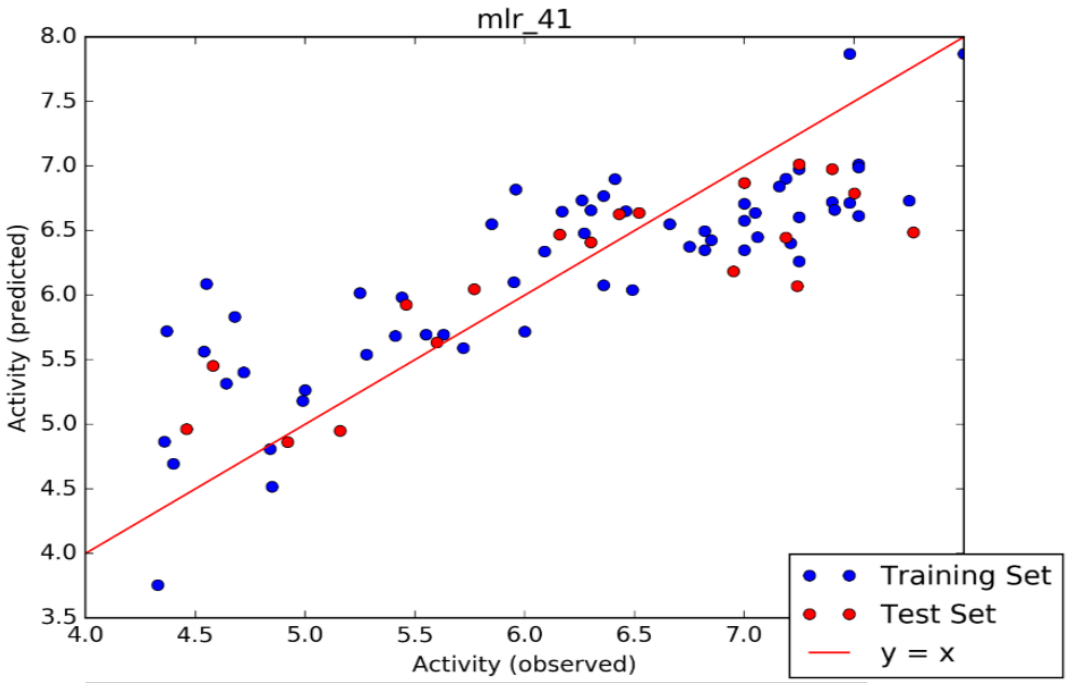

Training Set		Test Set	
S.D	R^2	RMSE	Q^2
0.6228	0.6852	0.5814	0.6691

Figure 10: Scatter plots of the constructive model with its statistical parameters

Table 5: Output data from external validation of the constructed model

Test	Data	Observed Value	Acceptable value
Model biasness test	nPE / Nne	2.0	<5
	nNE / Npe	0.5	<5
	|MPE / MNE|	1.0074	<2
	|MNE / MPE|	0.9455	<2
	AAE - |AE|	0.2356	>0.5
	R^2 (Residuals; serial correlation)	0.0342	<0.5
	R^2 (Residuals and observed response values)	0.1134	<0.5
Classical Metrics (for 100% data)			
	R^2(Test)	0.9710	Close to 1.0
	R0^2(Test)	0.9742	Close to 1.0
	Q2F1	0.9714	>0.6
	Q2F2	0.9677	>0.6
	Scaled Avg.Rm^2	0.9659	>0.6
	Scaled DeltaRm^2	0.0178	-

Preprints (www.preprints.org) | NOT PEER-REVIEWED | Posted: 20 December 2021 doi:10.20944/preprints202112.0296.v1

	CCC	0.9932	>0.85
Classical Metric (after removing 5% data with high residuals)	R^2Test(95% data)	0.9754	Close to 1.0
	R0^2Test(95% data)	0.9711	Close to 1.0
	Reverse R0^2Test(95% data)	0.9832	Close to 1.0
	Q2F1(95% data)	0.9811	>0.6
	Q2F2(95% data)	0.9732	>0.6
	ScaledAvgRm2(95% data)	0.9733	-
	ScaledDeltaRm2(95% data)	0.0098	-
	CCC(95% data)		>0.85
Error-based metrics	RMSEP(100% data)	0.3564	Close to 0.00
	SD(100% data)	0.2673	Close to 0.00
	MAE(100% data)	0.3239	Close to RMSEP
Error-based metric with high residuals)	RMSEP(95% data)	0.3599	>0.85
	SD(95% data)	0.2364	Close to 0.00
	MAE(95% data)	0.2546	Close to 0.00
Threshold acceptability indices	Data structure information	MAE :0.2821 MAE+3*SD:0.9528	MAE ≤ (0.15*Training set range) MAE+3*SD ≤(0.25*Training set range)
	0.1*Training set range :0.395 0.15*Training set range:0.5925 0.2*Training set range :0.79 0.25*Training set range:0.9875		

*****MAE: Mean absolute error, AAE: Average of absolute prediction errors; AE: Average of predictions errors; ABS: Absolute value, MPE: Mean of positive error; MNE: Mean of negative errors; ABS: Absolute value, NPE: Number of positive errors, NNE: Number of negative errors, CCC: Concordance correlation coefficient, RMSEP: Root mean square error of prediction

In summary, this study applied both computationally expensive (Fragment based drug design, IFD and Quantum mechanics) and non-expensive methods (Molecular docking, binding free energy, 2D QSAR, and ADMET parameters) to design a new set of compounds from fragments of known experimental inhibitors of *Pf*DODH. After the new compounds underwent thorough filtering using docking analysis, post-docking analysis, GI absorption, solubility and different rules for predicting drug-likeness, six compounds were chosen as the lead compounds. Structural investigation of these compounds showed that five of the compounds had [1, 2, 4,] triazolo [1, 5-a] pyrimidin-7-amine moieties as backbone structure, which is the same as backbone structure of the most promising experimental compounds against *Pf*DODH in different phases of clinical trials. Further computational techniques were applied to understand their mechanism of interaction with *Pf*DODH, toxicities, and pharmacokinetic properties of these 6 compounds. It

was demonstrated that the six compounds interacted with important residues responsible for the inhibition of the protozoa enzyme, and they had moderate pharmacokinetics properties. However, after investigating their toxicological properties, the drug-like compounds YME003, YME006, YME007 and YME009 are safer than the others, including the standard inhibitors. The DFT calculation revealed that YME003 is the most chemically reactive compounds, and YME002 is the most chemically inert compounds. The global descriptors help to determine the atomic portion of the compounds prone to nucleophilic and electrophilic attack. Finally, the compounds' bioactivity prediction using a well validated 2D QSAR further confirms their inhibitory activity against *Pf*DODH.

Conclusion

This study concludes that the newly designed compounds from the fragments of active *Pf*DODH can provide a new perspective into the design and development of drugs that can serve as inhibitors of *Pf*DODH.

Declarations of competing interest

The authors declare that they have no known competing financial interests or personal relationships that could have appeared to influence the work reported in this paper. The authors declare the following financial interests/personal relationships which may be considered as potential competing interests:

Funding

This research received no external financial or non-financial supports.

Authors contribution

OI: Generation and analysis of data, interpretation of data, preparation of manuscript draft and approval of manuscript for submission. OOE: Substantial manuscript revision, project supervision and provision of resources for research and approval of manuscript for submission. FO: Project design, data acquisition, preparation of manuscript draft and approval of manuscript for submission. POC: Data analysis, data interpretation, and approval of manuscript for submission. KB: Project design, manuscript draft, substantial manuscript

revision and approval of manuscript for submission. IMF: Substantial manuscript revision, project supervision and provision of resources for research and approval of manuscript for submission. All authors have read and approved the manuscript for submission

Acknowledgements

The authors acknowledge the technical support received from Computational Biologists at Bioinformatics and Molecular Biology Unit, Department of Biochemistry, Federal University of Technology, Akure, Ondo State, Nigeria**.**

References

1. Breman, J.G.; Egan, A.; Keusch, G.T. The intolerable burden of malaria: a new look at the numbers. *Am. J. Trop. Med. Hyg.* **2001**, *64*, iv–vii, doi:10.4269/ajtmh.2001.64.iv.
2. Belete, T.M. Recent Progress in the Development of New Antimalarial Drugs with Novel Targets. *Drug Des. Devel. Ther.* **2020**, *14*, 3875–3889, doi:10.2147/DDDT.S265602.
3. Organization, W.H. *World malaria report 2015*; World Health Organization, 2016; ISBN 9241565152.
4. Calderón, F.; Wilson, D.M.; Gamo, F.-J. Antimalarial drug discovery: recent progress and future directions. *Prog. Med. Chem.* **2013**, *52*, 97–151.
5. Kokwaro, G. Ongoing challenges in the management of malaria. *Malar. J.* **2009**, *8 Suppl 1*, S2, doi:10.1186/1475-2875-8-S1-S2.
6. Howitt, P.; Darzi, A.; Yang, G.-Z.; Ashrafian, H.; Atun, R.; Barlow, J.; Blakemore, A.; Bull, A.M.J.; Car, J.; Conteh, L.; et al. Technologies for global health. *Lancet (London, England)* **2012**, *380*, 507–535, doi:10.1016/S0140-6736(12)61127-1.
7. Veiga, M.I.; Ferreira, P.E.; Jörnhagen, L.; Malmberg, M.; Kone, A.; Schmidt, B.A.; Petzold, M.; Björkman, A.; Nosten, F.; Gil, J.P. Novel polymorphisms in Plasmodium falciparum ABC transporter genes are associated with major ACT antimalarial drug resistance. *PLoS One* **2011**, *6*, e20212, doi:10.1371/journal.pone.0020212.
8. Saralamba, S.; Pan-Ngum, W.; Maude, R.J.; Lee, S.J.; Tarning, J.; Lindegårdh, N.;

Chotivanich, K.; Nosten, F.; Day, N.P.J.; Socheat, D.; et al. Intrahost modeling of artemisinin resistance in Plasmodium falciparum. *Proc. Natl. Acad. Sci. U. S. A.* **2011**, *108*, 397–402, doi:10.1073/pnas.1006113108.

9. Mok, S.; Imwong, M.; Mackinnon, M.J.; Sim, J.; Ramadoss, R.; Yi, P.; Mayxay, M.; Chotivanich, K.; Liong, K.-Y.; Russell, B.; et al. Artemisinin resistance in Plasmodium falciparum is associated with an altered temporal pattern of transcription. *BMC Genomics* **2011**, *12*, 391, doi:10.1186/1471-2164-12-391.

10. Fidock, D.A.; Rosenthal, P.J.; Croft, S.L.; Brun, R.; Nwaka, S. Antimalarial drug discovery: efficacy models for compound screening. *Nat. Rev. Drug Discov.* **2004**, *3*, 509–520, doi:10.1038/nrd1416.

11. Oyelade, J.; Isewon, I.; Aromolaran, O.; Uwoghiren, E.; Dokunmu, T.; Rotimi, S.; Aworunse, O.; Obembe, O.; Adebiyi, E. Computational Identification of Metabolic Pathways of Plasmodium falciparum using the k-Shortest Path Algorithm. *Int. J. Genomics* **2019**, *2019*, 1750291, doi:10.1155/2019/1750291.

12. Vaidya, A.B.; Mather, M.W. Mitochondrial evolution and functions in malaria parasites. *Annu. Rev. Microbiol.* **2009**, *63*, 249–267, doi:10.1146/annurev.micro.091208.073424.

13. Phillips, M.A.; Rathod, P.K.; Rueckle, T.; Matthews, D.; Burrows, J.N.; Charman, S.A. Medicinal Chemistry Case History: Discovery of the Dihydroorate Dehydrogenase Inhibitor DSM265 as an Antimalarial Drug Candidate. In *Case Histories in Recent Drug Discovery*; Elsevier Inc., 2017; pp. 544–557.

14. Fischer, G. Chapter One - Recent advances in 1,2,4-triazolo[1,5-a]pyrimidine chemistry. In; Scriven, E.F. V, Ramsden, C.A.B.T.-A. in H.C., Eds.; Academic Press, 2019; Vol. 128, pp. 1–101 ISBN 0065-2725.

15. Honda, T.; Ojima, I. 8 - Curious effects of fluorine on medicinally active compounds. In *Progress in Fluorine Science*; Seppelt, K.B.T.-T.C.W. of F.M., Ed.; Elsevier, 2021; Vol. 6, pp. 241–276 ISBN 978-0-12-819874-2.

16. Mandt, R.E.K.; Lafuente-Monasterio, M.J.; Sakata-Kato, T.; Luth, M.R.; Segura, D.; Pablos-Tanarro, A.; Viera, S.; Magan, N.; Ottilie, S.; Winzeler, E.A.; et al. In vitro

selection predicts malaria parasite resistance to dihydroorotate dehydrogenase inhibitors in a mouse infection model. *Sci. Transl. Med.* **2019**, *11*, doi:10.1126/scitranslmed.aav1636.

17. Phillips, M.A.; Gujjar, R.; Malmquist, N.A.; White, J.; El Mazouni, F.; Baldwin, J.; Rathod, P.K. Triazolopyrimidine-based dihydroorotate dehydrogenase inhibitors with potent and selective activity against the malaria parasite Plasmodium falciparum. *J. Med. Chem.* **2008**, *51*, 3649–3653, doi:10.1021/jm8001026.

18. Murphy, S.C.; Duke, E.R.; Shipman, K.J.; Jensen, R.L.; Fong, Y.; Ferguson, S.; Janes, H.E.; Gillespie, K.; Seilie, A.M.; Hanron, A.E.; et al. A Randomized Trial Evaluating the Prophylactic Activity of DSM265 Against Preerythrocytic Plasmodium falciparum Infection During Controlled Human Malarial Infection by Mosquito Bites and Direct Venous Inoculation. *J. Infect. Dis.* **2018**, *217*, 693–702, doi:10.1093/infdis/jix613.

19. Bissaro, M.; Sturlese, M.; Moro, S. The rise of molecular simulations in fragment-based drug design (FBDD): an overview. *Drug Discov. Today* **2020**, *25*, 1693–1701, doi:10.1016/j.drudis.2020.06.023.

20. Zoete, V.; Grosdidier, A.; Michielin, O. Docking, virtual high throughput screening and in silico fragment-based drug design. *J. Cell. Mol. Med.* **2009**, *13*, 238–248, doi:10.1111/j.1582-4934.2008.00665.x.

21. Wishart, D.S.; Feunang, Y.D.; Guo, A.C.; Lo, E.J.; Marcu, A.; Grant, J.R.; Sajed, T.; Johnson, D.; Li, C.; Sayeeda, Z.; et al. DrugBank 5.0: a major update to the DrugBank database for 2018. *Nucleic Acids Res.* **2018**, *46*, D1074–D1082, doi:10.1093/nar/gkx1037.

22. Pierce, A.C.; Rao, G.; Bemis, G.W. BREED: Generating novel inhibitors through hybridization of known ligands. Application to CDK2, p38, and HIV protease. *J. Med. Chem.* **2004**, *47*, 2768–2775, doi:10.1021/jm030543u.

23. Daina, A.; Michielin, O.; Zoete, V. SwissADME: a free web tool to evaluate pharmacokinetics, drug-likeness and medicinal chemistry friendliness of small molecules. *Sci. Rep.* **2017**, *7*, 1–13.

24. Banerjee, P.; Eckert, A.O.; Schrey, A.K.; Preissner, R. ProTox-II: a webserver for the

prediction of toxicity of chemicals. *Nucleic Acids Res.* **2018**, *46*, W257–W263, doi:10.1093/nar/gky318.

25. Gaulton, A.; Bellis, L.J.; Bento, A.P.; Chambers, J.; Davies, M.; Hersey, A.; Light, Y.; McGlinchey, S.; Michalovich, D.; Al-Lazikani, B.; et al. ChEMBL: a large-scale bioactivity database for drug discovery. *Nucleic Acids Res.* **2012**, *40*, D1100-7, doi:10.1093/nar/gkr777.

26. Roy, K.; Das, R.N.; Ambure, P.; Aher, R.B. Be aware of error measures. Further studies on validation of predictive QSAR models. *Chemom. Intell. Lab. Syst.* **2016**, *152*, 18–33.

27. Dahlin, J.L.; Nissink, J.W.M.; Strasser, J.M.; Francis, S.; Higgins, L.; Zhou, H.; Zhang, Z.; Walters, M.A. PAINS in the assay: chemical mechanisms of assay interference and promiscuous enzymatic inhibition observed during a sulfhydryl-scavenging HTS. *J. Med. Chem.* **2015**, *58*, 2091–2113, doi:10.1021/jm5019093.

28. Baell, J.; Walters, M.A. Chemistry: Chemical con artists foil drug discovery. *Nature* **2014**, *513*, 481–483, doi:10.1038/513481a.

29. Brenk, R.; Schipani, A.; James, D.; Krasowski, A.; Gilbert, I.H.; Frearson, J.; Wyatt, P.G. Lessons learnt from assembling screening libraries for drug discovery for neglected diseases. *ChemMedChem* **2008**, *3*, 435–444, doi:10.1002/cmdc.200700139.

30. Lipinski, C.A.; Lombardo, F.; Dominy, B.W.; Feeney, P.J. Lead-and drug-like compounds: the rule-of-five revolution. Adv. **2001**.

31. Kikiowo, B.; Ogunleye, J.A.; Iwaloye, O.; Ijatuyi, T.T. Therapeutic potential of Chromolaena odorata phyto-constituents against human pancreatic α-amylase. *J. Biomol. Struct. Dyn.* **2020**, 1–12, doi:10.1080/07391102.2020.1833758.

32. Iwaloye, O.; Elekofehinti, O.O.; Kikiowo, B.; Fadipe, T.M.; Akinjiyan, M.O.; Ariyo, E.O.; Aiyeku, O.O.; Adewumi, N.A. Discovery of traditional Chinese medicine derived compounds as wild type and mutant Plasmodium falciparum dihydrofolate reductase inhibitors: Induced fit docking and ADME studies. *Curr. Drug Discov. Technol.* **2020**, doi:10.2174/1570163817999200729122753.

33. Onunkun*, A.T.; Elekofehinti, O.I. and O.O. Identification of Novel Nrf2 Activator via

Protein-ligand Interactions as Remedy for Oxidative Stress in Diabetes Mellitus. *Lett. Drug Des. Discov.* 2021, *18*, 1.

34. Singh, I.V.; Mishra, S. Molecular docking studies of benzamide derivatives for PfDHODH inhibitor as potent antimalarial agent. *Am J Biochem Molec Biol* **2019**, *9*, 1–6.

35. Haredi Abdelmonsef, A.; Eldeeb Mohamed, M.; El-Naggar, M.; Temairk, H.; Mohamed Mosallam, A. Novel Quinazolin-2,4-Dione Hybrid Molecules as Possible Inhibitors Against Malaria: Synthesis and in silico Molecular Docking Studies. *Front. Mol. Biosci.* **2020**, *7*, 105, doi:10.3389/fmolb.2020.00105.

36. Hoelz, L.V.; Calil, F.A.; Nonato, M.C.; Pinheiro, L.C.; Boechat, N. Plasmodium falciparum dihydroorotate dehydrogenase: a drug target against malaria. *Future Med. Chem.* **2018**, *10*, 1853–1874, doi:10.4155/fmc-2017-0250.

37. Deng, X.; Kokkonda, S.; El Mazouni, F.; White, J.; Burrows, J.N.; Kaminsky, W.; Charman, S.A.; Matthews, D.; Rathod, P.K.; Phillips, M.A. Fluorine modulates species selectivity in the triazolopyrimidine class of Plasmodium falciparum dihydroorotate dehydrogenase inhibitors. *J. Med. Chem.* **2014**, *57*, 5381–5394, doi:10.1021/jm500481t.

38. Oyinloye, B.E.; Iwaloye, O.; Ajiboye, B.O. Polypharmacology of Gongronema latifolium leaf secondary metabolites against protein kinases implicated in Parkinson's disease and Alzheimer's disease. *Sci. African* **2021**, e00826.

39. Nelson, D.R.; Zeldin, D.C.; Hoffman, S.M.G.; Maltais, L.J.; Wain, H.M.; Nebert, D.W. Comparison of cytochrome P450 (CYP) genes from the mouse and human genomes, including nomenclature recommendations for genes, pseudogenes and alternative-splice variants. *Pharmacogenetics* **2004**, *14*, 1–18, doi:10.1097/00008571-200401000-00001.

40. Olawale, F.; Olofinsan, K.; Iwaloye, O.; Emmanuel, T. Phytochemicals from Nigerian medicinal plants modulate therapeutically - relevant diabetes targets : insight from computational direction. *Adv. Tradit. Med.* **2021**, doi:10.1007/s13596-021-00598-z.

41. Kavitha, E.; Sundaraganesan, N.; Sebastian, S. Molecular structure, vibrational spectroscopic and HOMO, LUMO studies of 4-nitroaniline by density functional method. **2010**.

42. Subashchandrabose, S.; Saleem, H.; Erdogdu, Y.; Rajarajan, G.; Thanikachalam, V. FT-Raman, FT-IR spectra and total energy distribution of 3-pentyl-2, 6-diphenylpiperidin-4-one: DFT method. *Spectrochim. Acta Part A Mol. Biomol. Spectrosc.* **2011**, *82*, 260–269.

43. Jayaprakash, A.; Arjunan, V.; Mohan, S. Vibrational spectroscopic, electronic and quantum chemical investigations on 2,3-hexadiene. *Spectrochim. Acta. A. Mol. Biomol. Spectrosc.* **2011**, *81*, 620–630, doi:10.1016/j.saa.2011.06.064.

44. Ramya, N.; Jagadeeswari, P.; BIST, B. Proper coloring of regular graphs. *Int. J. Pure Appl. Math.* **2017**, *116*, 531–534.

45. Chinnasamy, S.; Selvaraj, G.; Kaushik, A.C.; Kaliamurthi, S.; Nangraj, A.S.; Selvaraj, C.; Singh, S.K.; Thirugnanasambandam, R.; Gu, K.; Wei, D. Identification of potent inhibitors against Aurora kinase A using molecular docking and molecular dynamics simulation studies. **2019**.

46. Kumar, V.; Roy, K. Development of a simple, interpretable and easily transferable QSAR model for quick screening antiviral databases in search of novel 3C-like protease (3CLpro) enzyme inhibitors against SARS-CoV diseases. *SAR QSAR Environ. Res.* **2020**, *31*, 511–526, doi:10.1080/1062936X.2020.1776388.